Aus der Medizinische Klinik mit Schwerpunkt Nephrologie
der Medizinischen Fakultät Charité – Universitätsmedizin Berlin

DISSERTATION

Knockout des von Hippel-Lindau Proteins im Nephron schützt vor akutem Nierenversagen

zur Erlangung des akademischen Grades
Doctor rerum medicinalium (Dr. rer. medic.)

vorgelegt der Medizinischen Fakultät
Charité – Universitätsmedizin Berlin

von

Susanne Mathia

aus Leipzig

Datum der Promotion: 27. Februar 2015

Inhaltsverzeichnis

1. Zusammenfassung

In akuten Nierenversagen (AKI) unterschiedlicher Genese finden sich Belege für eine regionale Hypoxie der Niere. In allen bisher untersuchten AKI-Modellen fand sich jedoch nur eine geringe und zeitlich begrenzte Hypoxieanpassung durch Hypoxie-induzierbare Transkriptionsfaktoren (HIF). Nephronsegmente mit dem höchsten Maße an morphologischen Zellschäden besitzen die geringste Fähigkeit zur HIF-Aktivierung. Präkonditionelle HIF-Aktivierung schützt vor AKI, dass mittels Klemmen der Nierenarterie oder des Nierenstiels erzeugt wird. Die Mechanismen dieser HIF-vermittelten Protektion sind weitgehend unbekannt. Ebenso bleibt unklar, ob solche Mechanismen auch in anderen AKI-Formen wirksam sein können. Die vorliegende Arbeit zeigt, dass eine selektive Hochregulation von HIF in Nierentubuli durch einen Pax8-rtTA-abhängigen und induzierbaren Knockout des von Hippel-Lindau Proteins (VHL) vor Rhabdomyolyse-induziertem AKI schützt. In diesem AKI-Modell ist die HIF-Aktivierung umgekehrt proportional dem tubulären Zellschaden, der in proximalen Tubuli zu 5% Nekrosen am Tag 1 und 40% Nekrosen am Tag 2 führt. Eine genomweite Microarray-Analyse zeigt, dass in diesem AKI-Modell etwa 20% des aktiven Genoms signifikant ($p<0,01$) reguliert ist. Rhabdomyolyse führt in VHL-KO-Mäusen in Vergleich zu Tieren ohne VHL-KO zu einer starken und anhaltenden HIF-Aktivierung in proximalen Tubuli. In den ersten 48h nach Auslösung der Rhabdomyolyse zeigt sich in VHL-KO-Tieren eine Nephroprotektion anhand niedrigerer Werte für Plasmakreatinin/Plasmaharnstoff, Caspase-3-Protein und Tubulusnekrose. Am Tag 1 nach Auslösung der Rhabdomyolyse ist der tubuläre Schaden größtenteils sublethal und daher potentiell reversibel. Zu diesem Zeitpunkt finden wir in VHL-KO-Tieren Hinweise für aktivierte Glykolyse und Glukoseaufnahme, Autophagie, Gefäßerweiterung und Protonenelimination, wie anhand von qPCR, Pathway-Enrichment-Analyse und Immunhistochemie ersichtlich. Zusammenfassend unterstützen unsere Daten die Ansicht, dass die HIF-bedingte AKI-Protektion auf einer Umstellung des Metabolismus hin zu einer anaeroben Energiegewinnung gründet.

2. Abstract

Regional renal hypoxia is a common feature of acute kidney injury (AKI) of different causes. However, in all AKI models tested so far, adaptation to hypoxia through hypoxia-inducible transcription factors (HIF) is very limited. Moreover, renal cell types most prone to injury seem to have the least capacity of up-regulating HIF under the respective AKI condition. Pre-conditional HIF activation has been demonstrated to protect from AKI induced by ischemia-reperfusion injury. But, the mechanisms responsible for renal protection are largely unknowns. Equally, it remains unclear if HIF based rescue mechanisms can be effective in other AKI forms, as well. The present work shows that selective HIF activation in renal tubules through Pax8-rtTA based inducible knockout of von Hippel-Lindau protein (VHL) protects from rhabdomyolysis-induced AKI. In this model, HIF activation inversely correlates with tubular injury, leading to 5% necrosis at d1 and 40% necrosis at d2 compared with controls. Genome wide microarray analysis reveals that roughly 20% of the active genome is significantly ($p<0.01$) regulated in this AKI form. Compared with control animals, VHL-KO mice subjected to rhabdomyolysis substantially activate HIF in portions of the nephron at risk for acute injury. In the first 48 h after induction of rhabdomyolysis, in VHL-KO mice kidney protection is reflected by lower plasma creatinine/urea, caspase-3 protein, and tubular necrosis. At d1 after rhabdomyolysis tubular injury is mostly sublethal, and hence, potentially reversible. We provide evidence that at this time point VHL-KO leads to activated glycolysis, enhanced cellular glucose uptake and utilization, autophagy, vasodilation, and proton removal, as demonstrated by qPCR, pathway enrichment analysis and immunohistochemistry. In conclusion, our data support the view that HIF based protection from AKI relies on a shift of metabolism towards anaerobic energy supply.

3. Eidesstattliche Versicherung

„Ich, Susanne Mathia, versichere an Eides statt durch meine eigenhändige Unterschrift, dass ich die vorgelegte Dissertation mit dem Thema: ‚Knockout des von Hippel-Lindau Proteins im Nephron schützt vor akutem Nierenversagen' selbstständig und ohne nicht offengelegte Hilfe Dritter verfasst und keine anderen als die angegebenen Quellen und Hilfsmittel genutzt habe.

Alle Stellen, die wörtlich oder dem Sinne nach auf Publikationen oder Vorträgen anderer Autoren beruhen, sind als solche in korrekter Zitierung (siehe „Uniform Requirements for Manuscripts (URM)" des ICMJE -*www.**icmje**.org*) kenntlich gemacht. Die Abschnitte zu Methodik (insbesondere praktische Arbeiten, Laborbestimmungen, statistische Aufarbeitung) und Resultaten (insbesondere Abbildungen, Graphiken und Tabellen) entsprechen den URM (s.o) und werden von mir verantwortet.

Mein Anteil an der ausgewählten Publikation entspricht dem, der in der untenstehenden gemeinsamen Erklärung mit dem/der Betreuer/in, angegeben ist.

Die Bedeutung dieser eidesstattlichen Versicherung und die strafrechtlichen Folgen einer unwahren eidesstattlichen Versicherung (§156,161 des Strafgesetzbuches) sind mir bekannt und bewusst."

_____

Datum Unterschrift

4. Ausführliche Anteilserklärung an der erfolgten Publikation

Publikation: Fähling M, **Mathia S**, Paliege A, Koesters R, Mrowka R, Peters H, Persson PB, Neumayer HH, Bachmann S, Rosenberger C. Tubular von Hippel-Lindau knockout protects against rhabdomyolysis-induced AKI. J Am Soc Nephrol. 2013
M.F. and S.M. contributed equally to this work.

Beitrag im Einzelnen:

Planung und Organisation der Tierversuche; Betreuung der Mäuse im laufenden Versuch; Blutabnahme aus dem Wangenplexus und Aufarbeitung der Proben zur Analyse von Plasma-Kreatinin und -Harnstoff im Zentrallabor der Charité; subkutane Injektion von Doxycyclin; intramuskuläre Injektion von Glycerin in die Hintergliedmaßen unter Isofluran-Narkose; Entnahme von Organen für weiterführende Analysen; Perfusionsfixierung der Nieren zur immunhistochemischen Analyse; Weiterverarbeitung des Gewebes mittels Entwässerungsautomat; Einbetten des Gewebes in Paraffin; dünne Gewebeschnitte mittels Mikrotom; Aufziehen der Schnitte auf einen Objektträger; Standardfärbungen der Schnitte wie HE-Färbung und PAS-Färbung; hoch-amplifizierende Immunhistochemie mittels spezifischer Antikörper an Paraffinschnitten; Recherche nach geeigneten Antikörpern; Anpassen der Färbeprotokolle an die Bedürfnisse des jeweiligen Antikörpers; Fotografieren repräsentativer Objektausschnitte mittels Durchlichtmikroskopie, Fluoreszenz-Mikroskopie oder mittels differentiellem Interferenzkontrast; semiquantitative Auswertung der Signale aus der Immun-histochemie; statistische Analysen; Literaturrecherche; wesentlicher Anteil am Studiendesign und der Manuskriptgestaltung.

Unterschrift, Datum und Stempel des betreuenden Hochschullehrers/der betreuenden Hochschullehrerin

_____

Unterschrift des Doktoranden/der Doktorandin

_____

ISI Web of Knowledge℠

Journal Citation Reports®

WELCOME | HELP

2012 JCR Science Edition

Journal Summary List

Journal Title Changes

Journals from: subject categories UROLOGY & NEPHROLOGY VIEW CATEGORY SUMMARY LIST

Sorted by: Impact Factor SORT AGAIN

Journals 1 - 20 (of 73) [1 | 2 | 3 | 4] **Page 1 of 4**

MARK ALL | UPDATE MARKED LIST

Ranking is based on your journal and sort selections.

Mark	Rank	Abbreviated Journal Title (linked to journal information)	ISSN	JCR Data						*Eigenfactor*® Metrics	
				Total Cites	Impact Factor	5-Year Impact Factor	Immediacy Index	Articles	Cited Half-life	*Eigenfactor*® Score	*Article Influence*® Score
☐	1	EUR UROL	0302-2838	17088	10.476	8.083	4.043	211	4.5	0.05462	2.393
☐	2	J AM SOC NEPHROL	1046-6673	30132	8.987	8.477	2.051	195	7.2	0.06912	2.985
☐	3	NAT REV NEPHROL	1759-5061	1354	7.943	7.409	1.206	63	2.3	0.00780	2.613
☐	4	KIDNEY INT	0085-2538	38094	7.916	6.968	2.603	234	8.6	0.06527	2.435
☐	5	AM J KIDNEY DIS	0272-6386	19101	5.294	5.417	1.724	199	8.6	0.03855	1.933
☐	6	CLIN J AM SOC NEPHRO	1555-9041	8449	5.068	5.445	1.100	240	3.4	0.04497	1.917
☐	7	NAT REV UROL	1759-4812	825	4.793	4.677	0.707	58	2.5	0.00474	1.625
☐	8	CURR OPIN NEPHROL HY	1062-4821	2923	3.964	3.763	0.795	83	5.6	0.00917	1.336
☐	9	PROSTATE	0270-4137	7036	3.843	3.410	0.713	188	6.6	0.01613	1.011
☐	10	J UROLOGY	0022-5347	45595	3.696	3.914	0.661	598	8.9	0.08059	1.252
☐	11	UROL ONCOL-SEMIN ORI	1078-1439	2140	3.647	3.082	0.490	143	3.6	0.00822	0.945
☐	12	AM J PHYSIOL-RENAL	1931-857X	17281	3.612	3.894	0.789	346	7.2	0.03661	1.187
☐	13	J SEX MED	1743-6095	6064	3.513	3.077	0.656	337	3.2	0.01727	0.602
☐	14	NEPHROL DIAL TRANSPL	0931-0509	21264	3.371	3.416	0.808	684	6.1	0.05229	1.032
☐	15	BJU INT	1464-4096	16518	3.046	2.907	0.713	617	6.2	0.04215	0.921
☐	16	PEDIATR NEPHROL	0931-041X	6856	2.939	2.503	0.565	239	6.1	0.01620	0.711
☐	17	WORLD J UROL	0724-4983	2639	2.888	2.827	0.500	120	5.0	0.00744	0.819
☐	18	SEMIN NEPHROL	0270-9295	1962	2.828	2.854	0.652	66	6.9	0.00521	1.014
☐	19	PROSTATE CANCER P D	1365-7852	1175	2.811	2.259	0.483	58	5.1	0.00394	0.770
☐	20	NEUROUROL URODYNAM	0733-2467	3511	2.674	2.603	0.297	138	5.8	0.00890	0.741

MARK ALL | UPDATE MARKED LIST

Journals 1 - 20 (of 73) [1 | 2 | 3 | 4] **Page 1 of 4**

6. Publikation

BASIC RESEARCH www.jasn.org

Tubular von Hippel-Lindau Knockout Protects against Rhabdomyolysis-Induced AKI

Michael Fähling,* Susanne Mathia,† Alexander Paliege,†‡ Robert Koesters,§ Ralf Mrowka,‖ Harm Peters,† Pontus Börje Persson,* Hans-Hellmut Neumayer,† Sebastian Bachmann,‡ and Christian Rosenberger†

Departments of *Vegetative Physiology, †Nephrology and Renal Transplantation, and ‡Anatomy, Charité Universitaetsmedizin, Berlin, Germany; §Tenon Hospital, INSERM/Pierre and Marie Curie University, Paris, France; and ‖Department of Experimental Nephrology, Internal Medicine Clinic III, University Clinic of Jena, Jena, Germany

ABSTRACT

Renal hypoxia occurs in AKI of various etiologies, but adaptation to hypoxia, mediated by hypoxia-inducible factor (HIF), is incomplete in these conditions. Preconditional HIF activation protects against renal ischemia-reperfusion injury, yet the mechanisms involved are largely unknown, and HIF-mediated renoprotection has not been examined in other causes of AKI. Here, we show that selective activation of HIF in renal tubules, through Pax8-rtTA–based inducible knockout of von Hippel-Lindau protein (VHL-KO), protects from rhabdomyolysis-induced AKI. In this model, HIF activation correlated inversely with tubular injury. Specifically, VHL deletion attenuated the increased levels of serum creatinine/urea, caspase-3 protein, and tubular necrosis induced by rhabdomyolysis in wild-type mice. Moreover, HIF activation in nephron segments at risk for injury occurred only in VHL-KO animals. At day 1 after rhabdomyolysis, when tubular injury may be reversible, the HIF-mediated renoprotection in VHL-KO mice was associated with activated glycolysis, cellular glucose uptake and utilization, autophagy, vasodilation, and proton removal, as demonstrated by quantitative PCR, pathway enrichment analysis, and immunohistochemistry. In conclusion, a HIF-mediated shift toward improved energy supply may protect against acute tubular injury in various forms of AKI.

J Am Soc Nephrol 24: 1806–1819, 2013. doi: 10.1681/ASN.2013030281

No specific therapy is currently available for human AKI, a clinical entity of increasing incidence and high morbidity and mortality.[1–4] Rhabdomyolysis, one of the leading causes of AKI, develops after trauma, drug toxicity, infections, burns, and physical exertion.[5–8] The animal model using an intramuscular glycerol injection with consequent myoglobinuria is closely related to the human syndrome of rhabdomyolysis.[9] Experimental data demonstrate renal vasoconstriction,[9–15] tubular hypoxia,[15,16] normal or even reduced intratubular pressure,[9–11] as well as large variation in single nephron GFR.[10,11] Intratubular myoglobin casts, a histologic hallmark, seem not to cause tubular obstruction,[9–11] but rather scavenge nitric oxide[17,18] and generate reactive oxygen species[19] followed by vasoconstriction.

The traditional discrimination between ischemic and toxic forms of AKI has been challenged because an increasing amount of evidence suggests that renal hypoxia is a common denominator in AKI of different etiologies.[20] Pimonidazole adducts, which accumulate in tissues at oxygen tensions <10 mmHg,[21] have been demonstrated in various AKI forms.[16,22–24] During AKI, hypoxia-inducible factors (HIFs), which are mainly regulated by oxygen-dependent proteolysis, were found to be upregulated in different renal

Received March 24, 2013. Accepted May 29, 2013.

M.F. and S.M. contributed equally to this work.

Published online ahead of print. Publication date available at www.jasn.org.

Correspondence: Dr. Christian Rosenberger, Department of Nephrology and Renal Transplantation, Charité Universitaetsmedizin Berlin, Campus Mitte, Charitéplatz 1, 10117 Berlin, Germany. Email: christian.rosenberger@charite.de

tubular segments.[16,20,22,24,25] HIFs are heterodimers of a constitutive β subunit, HIF-β (ARNT), and one of three oxygen-dependent α-subunits, HIF-1α, HIF-2α, and HIF-3α. The α-β dimers bind to hypoxia-response elements (HREs) in the promoter-enhancer region of HIF target genes.[26–28] Although the 5′-RCGTG-3′ (R = A or G) core HRE appears >1 million times in the entire genome[29] and in >4000 promoter regions of validated genes,[30] a recent study demonstrated HIF binding in roughly 350 genes.[31] Multiple HIF-based biologic effects are known, and it is widely accepted that a broad panel of these promote cellular survival in a hostile and oxygen-deprived environment.[27–29] In all types of AKI tested thus far, HIF activation along the nephron correlates with tubular survival, and the cells most vulnerable to injury exhibit no or only very limited HIF activity.[20] This observation led to the concept of insufficient HIF-based hypoxic adaptation in AKI. Consequently, maneuvers of preconditional HIF activation are utilized to ameliorate AKI. Indeed, many of these attempts are successful but the majority are conducted in ischemia-reperfusion injury.[20] It is largely unclear whether HIF can rescue kidneys exposed to AKI forms other than ischemia-reperfusion injury, and it is unclear which HIF target genes are involved in AKI protection if so. In many tumors, constitutive HIF activation promotes anaerobic ATP production, a process known as the Warburg effect.[32]

von Hippel-Lindau protein (VHL) is a ubiquitin ligase engaged in the stepwise HIF-α degradation process, which constantly occurs during normoxia.[33] Inducible Pax8-rtTA–based knockout of VHL (VHL-KO) achieves strong, selective, and persistent upregulation of HIF in all nephron segments.[34] In this study, we use this transgenic technique in conjunction with rhabdomyolysis in mice to address two issues: (*1*) Does HIF activation through VHL-KO protect from rhabdomyolysis-induced AKI? (*2*) If so, what are the biologic mechanisms and HIF target genes that are responsible for renal protection against acute injury? We demonstrate that indeed VHL-KO mice are largely protected against rhabdomyolysis-induced AKI, and provide evidence for a metabolic shift toward anaerobic ATP generation as the central protective mechanism.

RESULTS

Renal Function

The protocol for animal treatment to activate HIF by VHL-KO and induce rhabdomyolysis-mediated AKI is shown in Figure 1.

Neither VHL-KO *per se* nor withdrawal of drinking water had any effect on renal function or histology in otherwise untreated animals (not shown). At day 0, AKI and VHL-KO/AKI animals had comparable serum creatinine of approximately 0.18 mg/dl^{-1} (Figure 2A), as well as serum urea of approximately 50 mg/dl^{-1} (Figure 2B). Compared with day 0, AKI mice had significantly higher serum creatinine (0.93 mg/dl^{-1}) and serum urea (283 mg/dl^{-1}) at day 1. At day 2, both parameters were lower than at day 1 (serum creatinine, 0.65 mg/dl^{-1}; serum urea, 190 mg/dl^{-1}), although not statistically

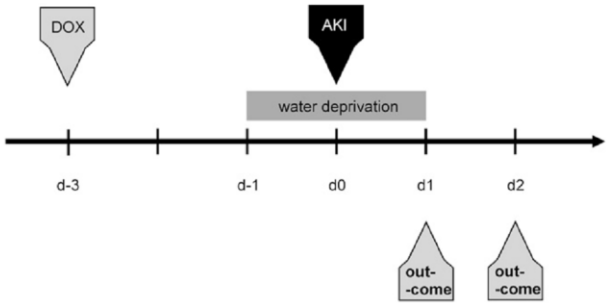

Figure 1. Protocol for AKI induction through rhabdomyolysis. AKI is induced under inhalation anesthesia by a single intramuscular injection of 50% glycerol into the left hind limb. Selective tubular HIF activation is induced by a single subcutaneous injection of doxycycline (DOX) 3 days before AKI induction. This time lag is necessary for establishment of maximum HIF activation *via* Pax8-rtTA–based knockout of VHL.

significant, but significantly higher than at day 0 (Figure 2). VHL-KO/AKI mice exhibited a similar time course of serum creatinine and urea. However, values were significantly lower than in the AKI group at both day 1 (serum creatinine, 0.28 mg/dl^{-1}; serum urea, 166 mg/dl^{-1}) and day 2 (serum creatinine, 0.25 mg/dl^{-1}; serum urea, 78 mg/dl^{-1}; Figure 2), reflecting functional protection.

Renal Morphology

AKI principally provoked three forms of injury in proximal tubules, as found in 0.5-μm semithin sections: vacuoles (arrows in Figure 3, A and B), cytoplasmic thinning (arrowheads in Figure 3, C and D), and tubular necrosis (curved arrows in Figure 3D). To reduce sampling error, time course and semiquantification of injury were performed in paraffin sections stained with periodic acid–Schiff, in which the major injury categories were detected equally reliable as in semithin sections. Injury progressed over time, with necrosis being rare at day 1 but prominent at day 2 (Figure 4, A and C). Visual inspection revealed that necrosis was less pronounced in VHL-KO/AKI compared with AKI (Figure 4, B and D). For semiquantification, non-necrotic changes, namely vacuoles and flattening, were counted together, as opposed to tubular necrosis. At day 1, no significant histologic difference was seen between AKI and VHL-KO/AKI (Figure 5). Necrosis appeared in <5% of proximal convoluted tubules (Figure 5A), but roughly 55% of these were remarkable for non-necrotic damage (Figure 5B). By contrast, AKI and VHL-KO/AKI differed significantly in the extent of necrosis (40% versus 20%; Figure 5A) and non-necrotic changes (20% versus 45%; Figure 5B) at day 2, suggesting morphologic protection by the knockout.

Apoptosis Marker Caspase-3

Apoptotic nuclei were rare in all four experimental groups (not shown). However, the apoptotic marker caspase-3 showed significant differences when measured by Western blot analysis

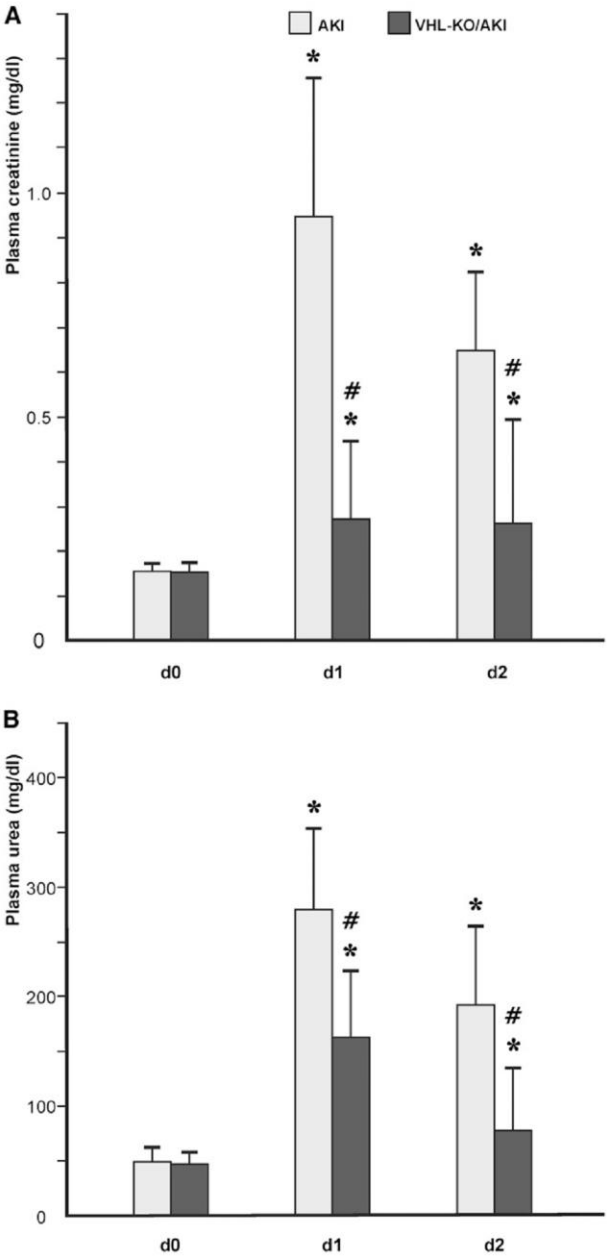

Figure 2. Tubular VHL knockout improves renal function during AKI. Both serum creatinine (A) and urea (B) are augmented at day 1 after induction of AKI. At day 2, both parameters decline, but are still elevated with respect to baseline. Animals with transgenic HIF activation in all renal tubules (VHL-KO/AKI, compare Figure 7B) exhibit less pronounced elevations of serum creatinine/urea than their littermates with scant and exclusively distal tubular HIF (AKI, compare Figure 7A). *$P<0.05$ versus control; #$P<0.05$ versus AKI.

(Figure 6). Both rhabdomyolysis groups had higher levels than controls or VHL-KO, respectively. In VHL-KO, caspase-3 levels were approximately 3-fold higher than in controls despite a

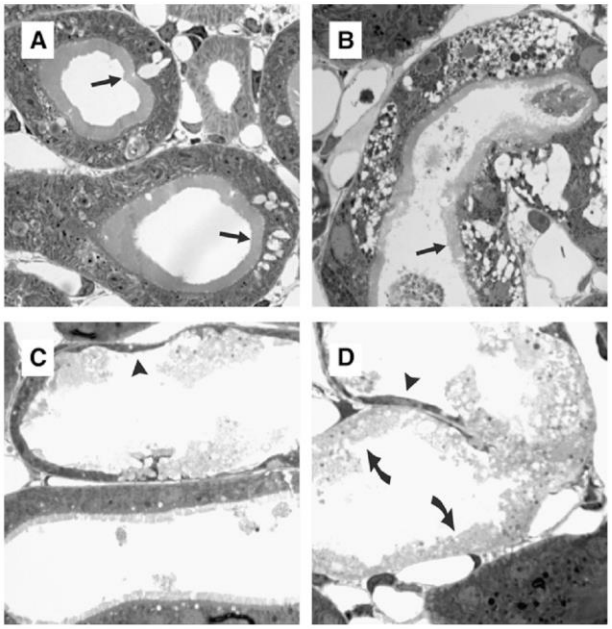

Figure 3. Tubular injury forms in rhabdomyolysis-induced AKI. Semithin plastic sections (0.5 μm). Arrow indicates vacuoles, arrowhead indicates cytoplasmic thinning, and curved arrow indicates necrosis. Tubular injury mainly affects proximal convoluted tubules. (A and B) Clear-cut, but non-necrotic, damage may occur under largely preserved brush border (arrows). (C) Largely normal and severely damaged tubules may occur side by side. (D) Different types of injury may coexist within the same tubular profile. Original magnification, ×1200.

similar histologic appearance. At day 1 after rhabdomyolysis, this relationship was inversed, with VHL-KO/AKI featuring significantly lower caspase-3 protein than AKI, suggesting that VHL-KO may have opposing effects depending on the underlying condition.

Cellular Location of HIF-α

We performed immunohistochemistry for HIF-1α and HIF-2α to test for activation of HIF (Figure 7, A and B, and Tables 1 and 2). As previously shown,[34] no signals were detectable in controls but appeared in all nephron segments in VHL-KO, with HIF-1α being more abundant than HIF-2α. AKI *per se* featured no HIF-2α staining (Table 2) but prominent HIF-1α immunosignals with increasing abundance from cortex to papilla, which is in line with known oxygen gradients,[35–37] suggesting hypoxic HIF activation (Table 1). Proximal tubules (asterisks in Figure 7A), the nephron segment most prone to injury in this model, had no detectable HIF-α, suggesting defective hypoxia adaptation. By contrast, proximal tubules exhibited prominent HIF-1α in VHL-KO/AKI (asterisks in Figure 7B) as did the remainder of nephron segments. Staining patterns were similar for days 1 and 2, except for some background in necrotic areas (not shown). HIF-2α was undetectable in VHL-KO/AKI.

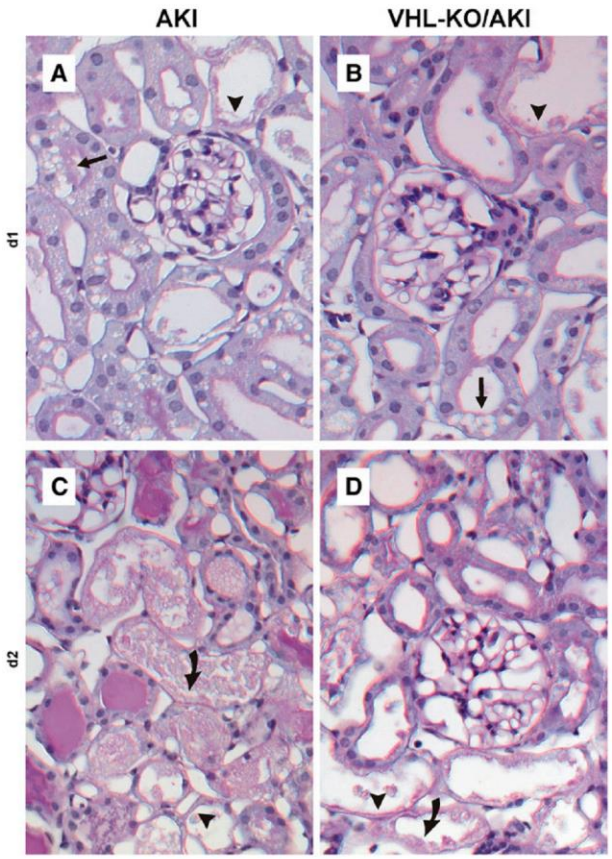

Figure 4. Tubular VHL knockout improves renal morphology during AKI. Paraffin sections (2 μm) stained with periodic acid–Schiff. Arrow indicates vacuoles, arrowhead indicates cytoplasmic thinning, and curved arrow indicates necrosis. Necrosis is rare at day 1 and is similar in AKI (A) and VHL-KO/AKI (B). By contrast, tubular necrosis is prominent at day 2, and is more extensive in AKI (C) than in VHL-KO/AKI (D). Original magnification, ×400.

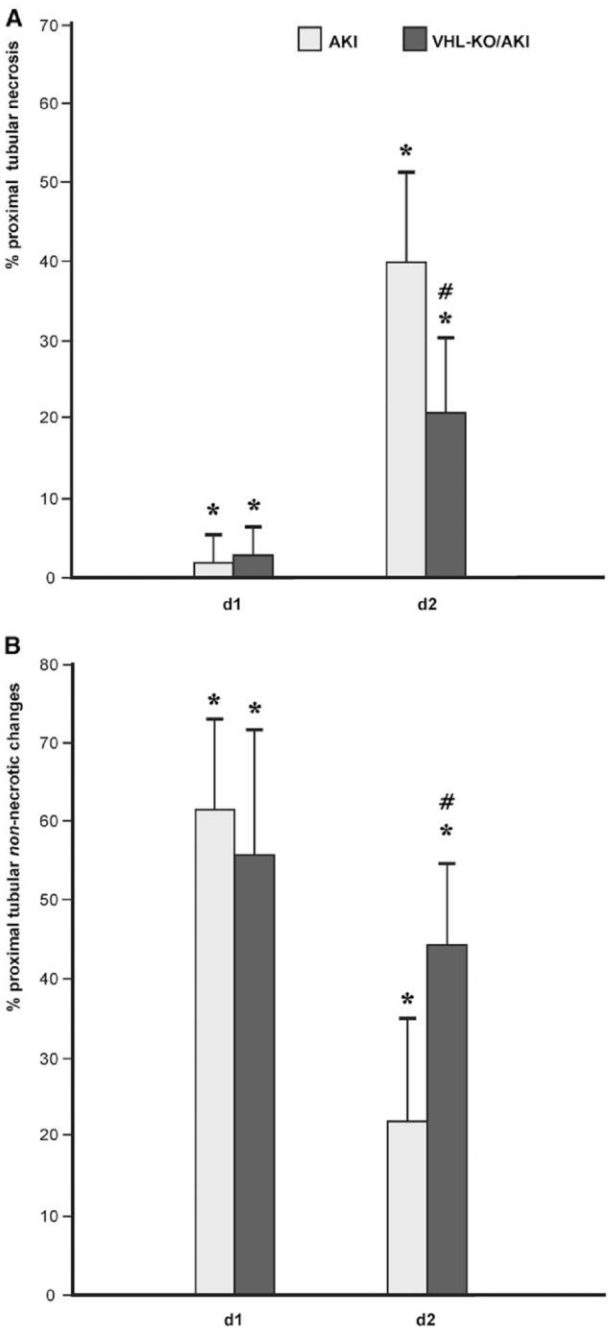

Figure 5. Semiquantification of injury in proximal tubules during AKI. At day 1 after AKI, induction tubular injury is mainly non-necrotic, and of similar extent in VHL-KO/AKI animals, which have marked HIF activation in all nephron segments (compare Figure 7B), as well as in AKI mice, which exhibit only scant HIF activation, and exclusively in largely unremarkable distal tubules (compare Figure 7A). By contrast, at day 2 after the onset of AKI, approximately 40% of proximal tubules are necrotic in AKI, and VHL-KO reduces this amount to 20%. *$P<0.05$ versus control; #$P<0.05$ versus AKI.

Genome-Wide Analyses

To gain an overview on the extent of gene regulation in the three interventional groups with respect to controls, we tested for the following: (*1*) present genes in controls (13,148 of 25,254 tested); (*2*) regulated genes (446 in VHL-KO, 2783 in AKI, and 2696 in VHL-KO/AKI) (Figure 8A); (*3*) upregulated genes (345 in VHL-KO, 1234 in AKI, and 1167 in VHL-KO/AKI) (Figure 8B); and (*4*) downregulated genes (101 in VHL-KO, 1549 in AKI, and 1529 in VHL-KO/AKI) (Figure 8C). Thus, AKI regulated approximately 20% of the active genome, and more than half of AKI-regulated genes were downregulated. Almost half of the genes regulated in VHL-KO/AKI were neither regulated by AKI nor by VHL-KO, suggesting that the combination of the two led to a unique transcriptome.

We performed real-time quantitative PCR (qPCR) and detected typical HIF target genes to verify microarray data as well as functional HIF activation by VHL-KO (Figure 9).

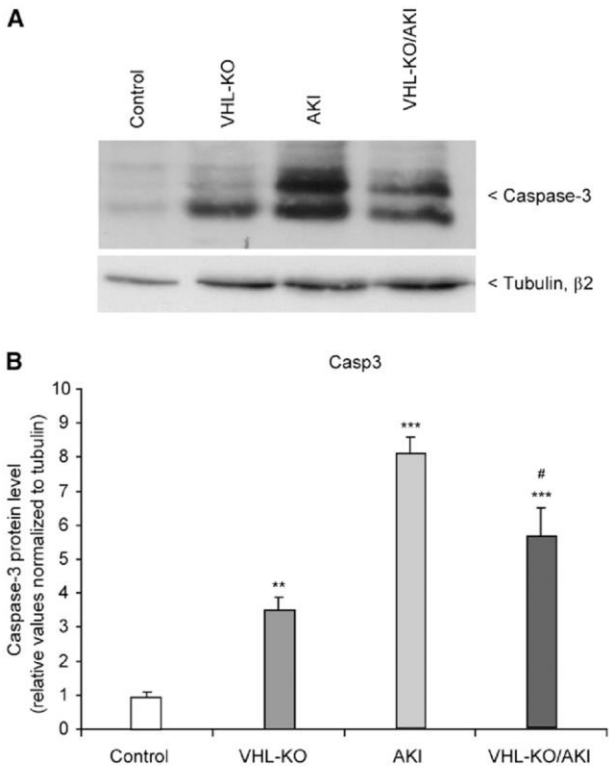

Figure 6. Tubular VHL knockout reduces caspase-3 during AKI. (A) Representative original Western blot of caspase-3 protein in mouse kidneys. Untreated controls are compared with VHL-KO, rhabdomyolysis-induced AKI, and VHL-KO/AKI. (B) Statistical analyses. n=5 per experimental group. $^{\#}P<0.05$ versus AKI; $^{**}P<0.01$ versus control; $^{***}P<0.001$ versus control.

Selected candidates are involved in crucial protective pathways such as glycolysis (aldolase-C/fructose-bisphosphatase [AldoC] and hexokinase-2 [Hk2]),[32,38] glucose uptake (solute carrier family 2 member 1 [Slc2a1 alias Glut-1][39]), proton excretion (carbonic anhydrase-9 [Car-9][40]), vasodilation (adrenomedullin, Adm[41]), and scavenging of free radicals (heme oxygenase (decycling) 1 [Hmox-1][42]).

We found a good correlation between microarray and qPCR data. All tested HIF target genes were elevated at the transcript level by VHL-KO as determined by qPCR. By contrast, in rhabdomyolysis the HIF target genes Car-9 and AldoC were unchanged, or even depressed with respect to untreated controls. This finding backs the hypothesis of insufficient HIF response despite of renal hypoxia during AKI.

Pathway Enrichment Analyses

In tumors, stable HIF activation is responsible for the Warburg effect.[32] We hypothesized that key enzymes of anaerobic energy metabolism will be upregulated in kidneys of Pax8-rtTA–based VHL-KO mice. Indeed, pathway enrichment analysis

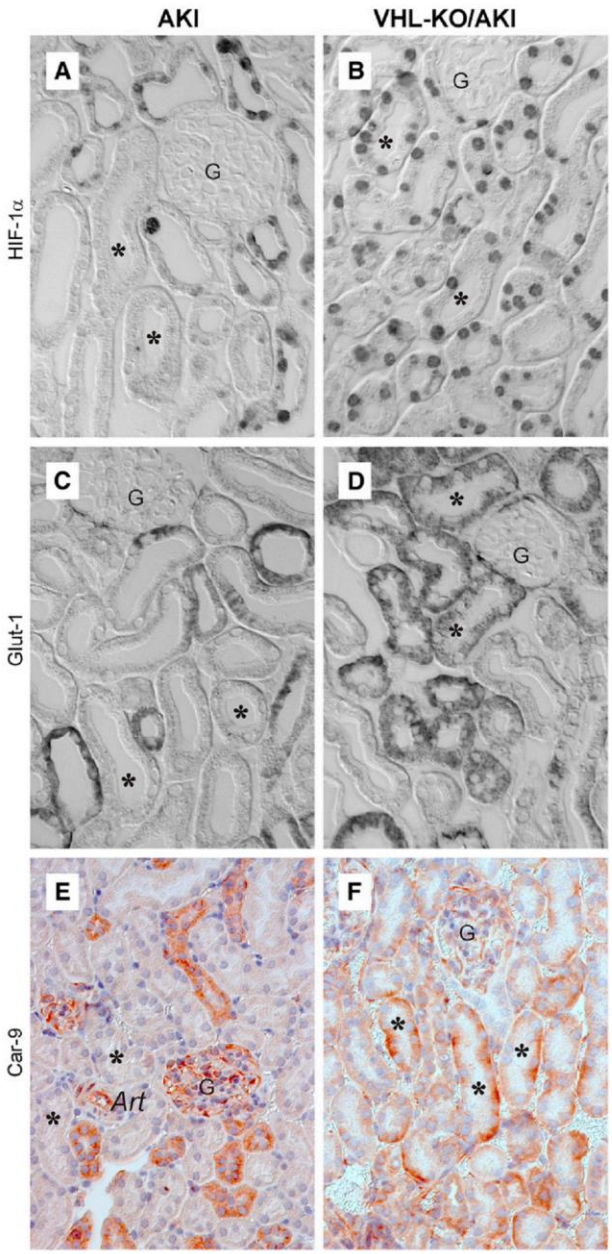

Figure 7. VHL knockout induces HIF-1α and the HIF target genes Glut-1 and Car-9 in tubules at risk for injury. Immunohistochemistry at day 1 after induction of AKI. At this time point, histologic injury is mainly of the non-necrotic type and is comparable in AKI and VHL-KO/AKI (compare Figure 5). AKI features HIF-1α (A), Glut-1 (C), and Car-9 (E) in distal but not in proximal tubules. By contrast, VHL-KO/AKI reveals all three immunosignals in proximal tubules (asterisks in B, D, and F). Art, arteriole; asterisk, proximal tubule; G, glomerulus. Original magnification, ×400 in A–D; ×250 in E and F.

Table 1. HIF-1α immunoreactivity at day 1 after AKI

Renal Zone	Cell Type	Control[a]	AKI[b]	VHL-KO[c]	VHL-KO/AKI[d]
Cortex, labyrinth	Proximal convoluted tubule	—	+	+++	++
	Thick ascending limb	—	++	+++	+++
	Distal convoluted tubule	—	—	+++	+++
	Connecting tubule	—	—	+++	+++
	Tubular-interstitial cell	—	—	—	—
Cortex, medullary ray	Proximal tubule (S3)	—	+	+++	++
	Thick ascending limb	—	++	+++	+++
	Collecting duct	—	++	+++	+++
	Tubular-interstitial cell	—	—	—	—
Outer stripe of outer medulla	Proximal tubule (S3)	—	—	+++	++
	Collecting duct	—	+	+++	+++
	Thick ascending limb	—	++	+++	+++
	Tubular-interstitial cell	—	—	—	—
Inner stripe of outer medulla	Thick ascending limb	—	++	+++	+++
	Thin limb	—	+	+++	+++
	Collecting duct	—	++	+++	+++
	Tubular-interstitial cell	—	+	—	++
Inner medulla and papilla	Collecting duct	—	++	+++	+++
	Thin limb	—	+	+++	+++
	Tubular-interstitial cell	—	+	—	—

[a]Untreated animals.
[b]Intramuscular glycerol injection at day 0.
[c]Subcutaeneous doxycycline injection at day 3, which activates HIF in all nephron segments.
[d]Combination of Intramuscular glycerol injection at day 0 and subcutaneous doxycycline injection at day 3.

Table 2. HIF-2α immunoreactivity at day 1 after AKI

Renal Zone	Cell Type	Control[a]	AKI[b]	VHL-KO[c]	VHL-KO/AKI[d]
Cortex, labyrinth	Proximal convoluted tubule	—	—	++	—
	Thick ascending limb	—	—	++	—
	Distal convoluted tubule	—	—	++	—
	Connecting tubule	—	—	++	—
	Tubular-interstitial cell	—	—	—	—
Cortex, medullary ray	Proximal tubule (S3)	—	—	++	—
	Thick ascending limb	—	—	++	—
	Collecting duct	—	—	++	—
	Tubular-interstitial cell	—	—	—	—
Outer stripe of outer medulla	Proximal tubule (S3)	—	—	++	—
	Collecting duct	—	—	++	—
	Thick ascending limb	—	—	++	—
	Tubular-interstitial cell	—	—	—	—
Inner stripe of outer medulla	Thick ascending limb	—	—	+	—
	Thin limb	—	—	+	—
	Collecting duct	—	—	+	—
	Tubular-interstitial cell	—	—	—	—
Inner medulla and papilla	Collecting duct	—	—	+	—
	Thin limb	—	—	+	—
	Tubular-interstitial cell	—	—	—	—

[a]Untreated animals.
[b]Intramuscular glycerol injection at day 0.
[c]Subcutaneous doxycycline injection at day 3, which activates HIF in all nephron segments.
[d]Combination of intramuscular glycerol injection at day 0 and subcutaneous doxycycline injection at day 3.

revealed that compared with controls, the major effect of VHL-KO *per se* was activation of glycolysis and increased glucose utilization (Table 3). In AKI, the TNF-α/NF-κB pathway was the most significantly upregulated.

To prove our hypothesis that renal protection by VHL-KO is a shift toward oxygen-independent energy metabolism, we next compared rhabdomyolysis-induced AKI in knockout animals and controls (VHL-KO/AKI versus AKI). A total of 686

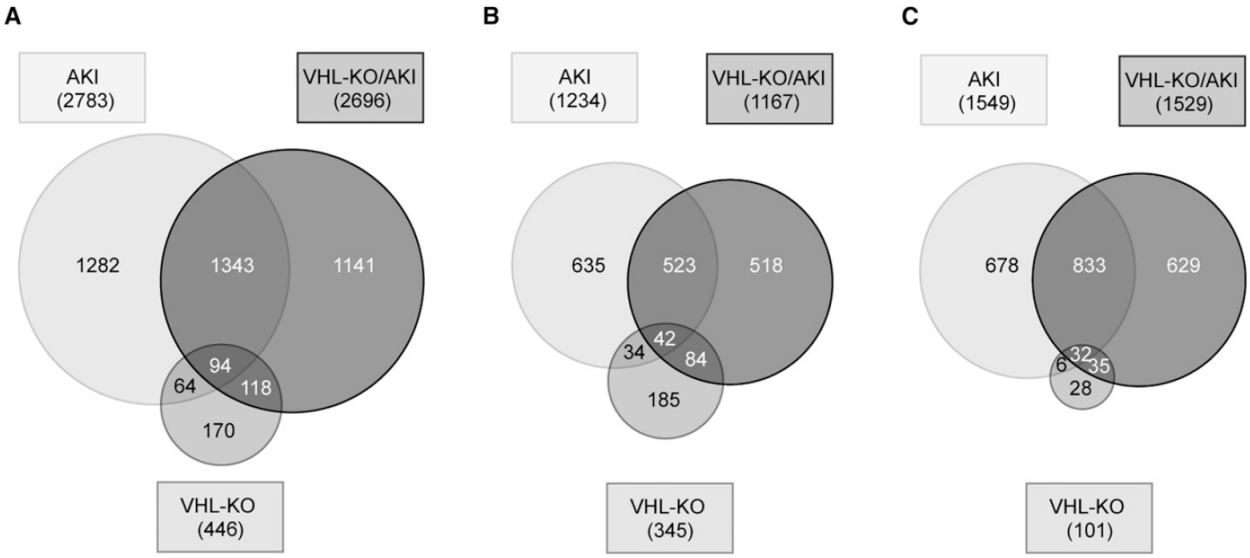

Figure 8. Tubular VHL knockout leads to a largely novel transcriptome during AKI. Venn diagram illustrating the number of significantly regulated candidates ($P<0.01$) in VHL-KO, AKI, or VHL-KO/AKI relative to controls, respectively (A). Separate illustration of upregulated (B) and downregulated candidates (C).

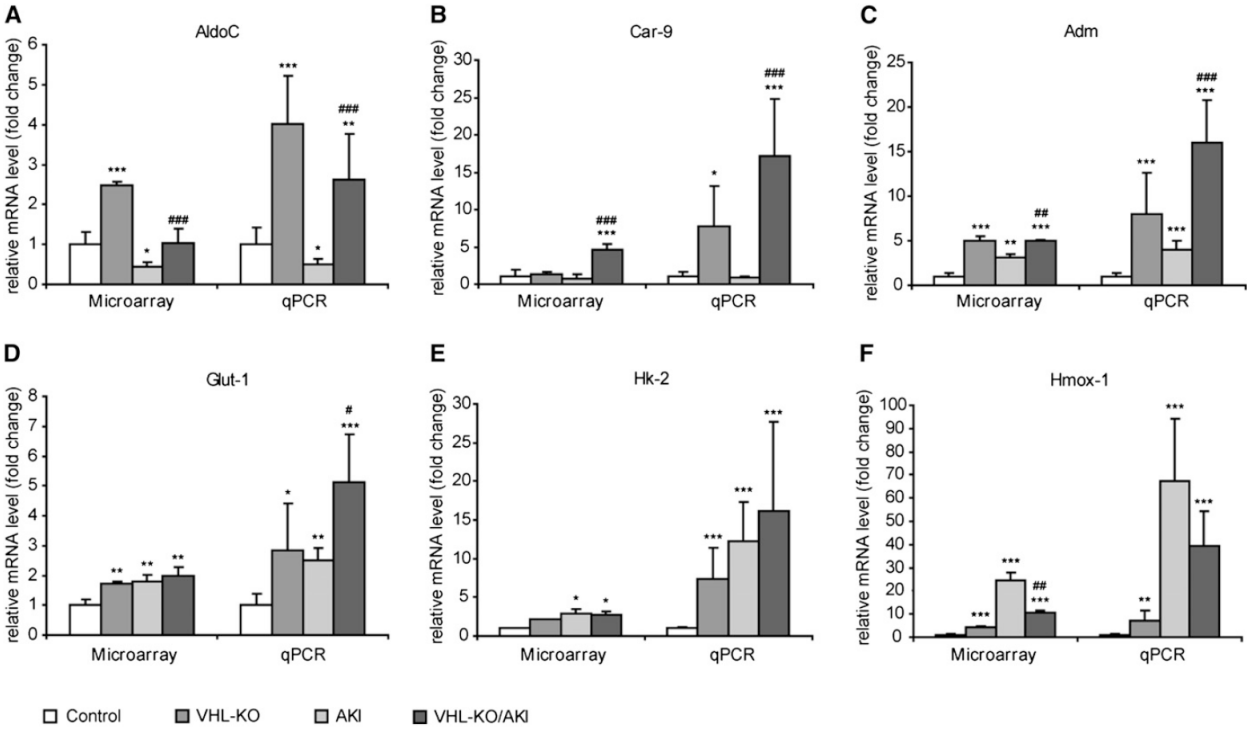

Figure 9. Tubular VHL knockout upregulates HIF target genes with cell-protective potential. Microarray analysis and qPCR are shown side by side. AKI and VHL-KO/AKI are shown at day 1 after induction of injury. $^{*}P<0.05$ versus control; $^{**}P<0.01$ versus control; $^{***}P<0.001$ versus control; $^{\#}P<0.05$ versus AKI; $^{\#\#}P<0.01$ versus AKI; $^{\#\#\#}P<0.001$ versus AKI.

candidates were differentially regulated, 476 of which were upregulated and 210 were downregulated. Indeed, the most prominent difference between VHL-KO/AKI and AKI was an enrichment of factors involved in glycolysis. By contrast, stress response and energy-consuming processes were reduced (Table 3).

We further compared the biologic roles of the top 30 upregulated and downregulated genes, respectively. Among the top 30 upregulated genes, there were 9 acknowledged HIF target genes, suggesting a high level of HIF-based transactivation. Six of these HIF target genes collectively achieved a shift toward anaerobic ATP production (Table 4). The main biologic roles of the top 30 downregulated genes in VHL-KO/AKI versus AKI are shown in Table 5. Twelve of these were hypoxia-regulated markers of tissue injury, repair, or remodeling, which is in line with a less severe tissue injury.

Location of HIF Target Genes in Tubules at Risk

To test whether HIF activation was accompanied by target gene transactivation in proximal tubules, we performed immunohistochemistry for the cell-protective HIF-1α target genes Glut-1 and Car-9. The cellular location of the latter has not

Table 3. Functional enrichment analysis at day 1 after AKI ($P<0.01$)

Group	Upregulated Pathways[a]	P	Downregulated Pathways[a]	P
VHL-KO versus control				
No. of genes[a]	326		93	
	Glycolysis and gluconeogenesis	2.47e-07	Glutathione metabolism	0.001
	ErbB signaling pathway	0.0002	Metabolic pathways	0.001
	Renal cell carcinoma	0.001	Folate biosynthesis	0.002
	MAPK signaling pathway	0.0002	Metapathway biotransformation	0.003
	B cell receptor signaling pathway	0.0003	Drug metabolism/cytochrome P450	0.004
	EGFR1 signaling pathway	0.001	Selenium	0.01
	Keap1-Nrf2	0.002	Folic acid network	0.01
	VEGF signaling pathway	0.02	AA metabolism	0.01
	Delta-notch signaling pathway	0.02	Oxidative stress	0.01
AKI versus control				
No. of genes[a]	1107		1421	
	TNF-α NF-κB signaling pathway	2.91e-12	Metabolic pathways	1.58e-15
	Proteasome degradation	5.54e-10	Oxidative phosphorylation	9.30e-05
	MAPK signaling pathway	1.43e-09	Biosynthesis of unsaturated fatty acids	0.0002
	EGFR1 signaling pathway	4.49e-09	Nuclear receptors	0.0003
	Spliceosome	9.29e-08	Electron transport chain	0.001
	Translation factors	1.00e-07	Steroid biosynthesis	0.002
	FAS pathway; stress induction of HSP regulation	1.55e-06	Glycosphingolipid biosynthesis (globo series)	0.004
	Toll-like receptor signaling pathway	3.16e-06	PG synthesis and regulation	0.01
	Insulin signaling	4.35e-06		
	Endocytosis	8.10e-06		
	Diurnally regulated genes with circadian orthologs	1.46e-05		
	Circadian exercise	1.46e-05		
	Neurotrophin signaling pathway	5.99e-05		
	Tight junction	0.001		
VHL-KO/AKI versus AKI				
No. of genes[a]	476		210	
	Glycolysis and gluconeogenesis	1.66e-09	Diurnally regulated genes with circadian orthologs	8.44e-05
	Statin pathway (PharmGKB)	9.11e-05	Adipogenesis	0.001
	Biotin metabolism	0.001	EGFR1 signaling pathway	0.001
	PPAR signaling pathway	0.001	Id signaling pathway	0.0003
	Glycogen metabolism	0.01	IL-1 signaling pathway	0.001
			Circadian exercise	0.001
			MAPK signaling pathway	0.001
			IL-2 signaling pathway	0.002

MAPK, mitogen-activated protein kinase; EGFR1, epidermal growth factor receptor 1; VEGF, vascular endothelial growth factor; FAS, TNF receptor superfamily member 6; HSP, heat shock protein; PPAR, peroxisome proliferator-activated receptor.
[a]Threshold P value <0.01.

been determined in the kidney thus far. As a positive control, we used paraffin-embedded mouse stomach, in which Car-9 is constitutively expressed.[43] Membranous signals indeed appeared in epithelial cells of the corpus with virtually no background (Supplemental Figure 1). In AKI, both Glut-1 and Car-9 (Figure 7, C and E) matched the staining pattern of controls (not shown). Signal distribution in VHL-KO/AKI (Figure 7, D and F) was largely equivalent to that observed in

Table 4. VHL-KO/AKI versus AKI at day 1, top 30 upregulated ($P<0.01$)

Gene	Symbol	Other Aliases	Fold Change	HIF Target Gene[a]	Induced in VHL-KO	Induced by Hypoxi[b]	RefSeq	Function/Remarks
Vomeronasal 1 receptor 32	Vmn1r32		31.71		Yes		NM_134170	Neural signaling
Vomeronasal 1 receptor 34	Vmn1r34		24.29		Yes		NM_001166719	Neural signaling
Vomeronasal 1 receptor 37	Vmn1r37		10.29		Yes		NM_134165	Neural signaling
Chemokine (C-C motif) ligand 28	Ccl28		8.29		No	Yes	NM_020279	Chemoattraction, Treg recruitment
Apoc-III	Apoc3		6.81		Yes		NM_023114	Lipid metabolism
Carbonic anhydrase 9	Car9	CA9	6.76	Yes	Yes	Yes	NM_139305	Ph regulation
IL 17 receptor B	Il17rb		6.43		Yes		NM_019583	NF-κB pathway
EGL nine homolog 3 (*Caenorhabditis elegans*)	Egln3	PHD3	6.37	Yes	Yes	Yes	NM_028133	Transcription
Apo A-IV	Apoa4		6.34		No		NM_007468	Lipid metabolism
Defensin β19	Defb19		5.97		No		NM_145157	Immunity
Phosphofructokinase, liver, B type	Pfkl	AldoC	4.70	Yes	Yes	Yes	NM_008826	Glycolysis
PRELI domain containing 2	Prelid2		4.19		Yes		NM_029942	Development
Pyruvate dehydrogenase kinase, isoenzyme 1	Pdk1		4.13	Yes	Yes	Yes	NM_172665	Krebs cycle inhibition
Solute carrier family 16 (monocarboxylic acid transporters)	Slc16a3		4.02		Yes	Yes	NM_001038653	Lactic acid and pyruvate transport
Cytochrome P450, family 4, subfamily a, polypeptide 14	Cyp4a14		3.84		No		NM_007822	AA metabolism, 20-HETE
3-hydroxy-3-methylglutaryl-CoA synthase 2	Hmgcs2		3.78		No		NM_008256	Ketogenesis
Angiopoietin-like 3	Angptl3	ANGPT5	3.41		Yes		NM_013913	Angiogenesis
BCL2/adenovirus E1B interacting protein 3	Bnip3	NIP3	3.25	Yes	Yes	Yes	NM_009760	Autophagy
Endothelin 3	Edn3	ET-3	3.12		Yes		NM_007903	Development
Lymphocyte antigen 6 complex, locus F	Ly6f		2.97		No		NM_008530	Unknown
Aldo-keto reductase family 1, member C18	Akr1c18		2.96		No		NM_134066	Steroid metabolism
Vomeronasal 1 receptor 20	Vmn1r20		2.87		No		NM_001101533	Unknown
IGF binding protein 1	Igfbp1		2.85	Yes	No	Yes	NM_008341	Insulin resistance
Adrenomedullin 2	Adm2		2.62	Yes	Yes	Yes	NM_182928	Decreased endothelial permeability
Phosphofructokinase, platelet	Pfkp	AldoC	2.54	Yes	Yes	Yes	NM_019703	Glycolysis
Hormonally upregulated Neu-associated kinase	Hunk		2.54		No		NM_015755	Constitutive in distal tubules; inhibits angiotensin II effect
Potassium inwardly-rectifying channel, subfamily J, 1	Kcnj1		2.49		No		NM_001168354	Mutation leads to Bartter syndrome
Flavin containing monooxygenase 5	Fmo5		2.45		No		NM_001161765	NADPH dependent
Solute carrier family 23 (nucleobase transporters), 3	Slc23a3		2.42		No		NM_194333	Orphan transporter
Phosphoenolpyruvate carboxykinase 1, cytosolic	Pck1	PEPCK	2.39	Yes	No	Yes	NM_011044	Gluconeogenesis

Treg, regulatory T cell; 20-HETE, 20-hydroxyeicosatetraeonic acid.
[a]HIF target genes: empty spaces are left for candidates without solid evidence for HIF-dependent regulation.
[b]Genes regulated by hypoxia: empty spaces are left for candidates without solid evidence for hypoxia-dependent regulation.

Table 5. VHL-KO/AKI versus AKI at day 1, top 30 downregulated ($P<0.01$)

Gene	Symbol	Other Aliases	Fold Change	HIF Target Gene[a]	Reduced in VHL-KO	Induced by Hypoxia[b]	RefSeq	Function/Remarks
G protein-coupled receptor, family C, group 5, member A	Gprc5a		0.31		No		NM_181444	Retinoic acid–dependent tumor suppressor
Growth arrest and DNA-damage-inducible 45α	Gadd45a		0.33		No	Yes	NM_007836	Cell cycle, DNA repair, tumor suppressor
Growth differentiation factor 15	Gdf15	PTGFB	0.34		No	Yes	NM_011819	Angiogenesis, transcription, activates HIF
Early growth response 1	Egr1		0.38		No	Yes	NM_007913	HIF cotranscription factor
Polo-like kinase 3 (*Drosophila*)	Plk3		0.39		No	Yes	NM_013807	Tumor suppressor, phosphorylates HIF
NADH dehydrogenase subunit 6	ND6		0.40		No		NC_005089	Mitochondrial gene of complex I, HIF-1α transcription
Stratifin	Sfn	YWHAS	0.40		No		NM_018754	Matrix turnover
Dual specificity phosphatase 5	Dusp5		0.43		No		NM_001085390	Dephosphorylate both tyrosine and serine/ threonine residues
PG-endoperoxide synthase 2	Ptgs2	COX2	0.44	Yes	No	Yes	NM_011198	PG synthesis, activates HIF
Cysteine-rich protein 61	Cyr61		0.44	Yes	No	Yes	NM_010516	Angiogenesis
Tumor-associated calcium signal transducer 2	Tacstd2		0.44		No		NM_020047	Membrane receptor
Rho family GTPase 3	Rnd3		0.44	Yes	No	Yes	NM_028810	Cytoskeleton, epithelial-mesenchymal transdifferentiation
Eph receptor A2	Epha2		0.45	Yes	No	Yes	NM_010139	Development
Transmembrane protein 108	Tmem108		0.47		No		NM_178638	Lipid metabolism
Coagulation factor III	F3	TF	0.48		No	Yes	NM_010171	Coagulation
IFN-related developmental regulator 1	Ifrd1		0.48		No	Yes	NM_013562	Transcription
Pleckstrin homology-like domain, family A, member 1	Phlda1		0.48		No		NM_009344	Apoptosis
Cholesterol 25-hydroxylase	Ch25h		0.48		No		NM_009890	Lipid metabolism
Choline kinase α	Chka		0.48	Yes	No	Yes	NM_013490	Biosynthesis of phosphatidylcholine
fos-like antigen 1	Fosl1		0.50		No	Yes	NM_010235	Transcription
Dual specificity phosphatase 14	Dusp14		0.51		No	Yes	NM_019819	Dephosphorylate both tyrosine and serine/ threonine residues
Retinoblastoma binding protein 6	Rbbp6		0.51		No		NM_011247	Cell cycle
Transgelin	Tagln		0.52		No		NM_011526	Cytoskeleton, shape change
Jun oncogene	Jun	AP-1	0.53		No	Yes	NM_010591	HIF cotranscription factor
Transmembrane protein 171	Tmem171		0.53		No		NM_001025606	Urate transport?
Thioredoxin reductase 1	Txnrd1		0.54		No		NM_001042523	ROS scavenging, downregulated in hypoxia
Suppressor of cytokine signaling 3	Socs3		0.55		No	Yes	NM_007707	Modulation of cytokine signaling
Nestin	Nes		0.55		No	Yes	NM_016701	Angiogenesis
Keratin 18	Krt18		0.56		No		NM_010664	Cancer
Dual specificity phosphatase 8	Dusp8		0.56		No	Yes	NM_008748	Dephosphorylates tyrosine *and* serine/threonine residues

ROS, reactive oxygen species.
[a]HIF target genes: empty spaces are left for candidates without solid evidence for HIF-dependent regulation.
[b]Genes regulated by hypoxia: empty spaces are left for candidates without solid evidence for hypoxia-dependent regulation.

VHL-KO (not shown). Moreover, both Glut-1 and Car-9 appeared in distal but not in proximal tubules (asterisks in Figure 7, C and E). By contrast, VHL-KO/AKI featured *de novo* expression in the basolateral membranes and adjacent cytoplasm of proximal convoluted tubules (asterisks in Figure 7D for Glut-1, and in Figure 7F for Car-9). Additional extratubular and constitutive expression was noted in glomeruli (Figure 7, C and E) including Glut-1 in Bowman's capsule and Car-9 in various cell types, which most likely include mesangial and endothelial cells. Moreover, constitutive Car-9 was expressed in endothelial cells and in myocytes of arterioles (Figure 7E).

DISCUSSION

Here we demonstrate protection against rhabdomyolysis-induced AKI by preconditional knockout of VHL. The latter is closely associated with a metabolic shift toward anaerobic ATP production.

Experimental rhabdomyolysis is intimately related to the human syndrome.[9] Our finding of nuclear HIF-1α protein accumulation in the largely unremarkable distal tubules, but not in the injured proximal tubules, indicates hypoxia with insufficient adaptation. Pax8-rtTA–based VHL-KO achieves selective and inducible HIF activation in the entire nephron, and significantly reduces serum creatinine/urea as well as tubular necrosis at day 2 after the onset of rhabdomyolysis.

Upregulation of several cell-protective HIF target genes suggests that the effect of VHL-KO is conferred through HIF. It is important to recognize that target gene specificity of the two major HIFα isoforms varies with respect to cell type and underlying condition.[44,45] Presumably, the setting in our VHL-KO mice is more or less matched by that of renal cell carcinoma cells with constitutive deletion of VHL,[44] in which Car-9 and Bnip3 are regulated by HIF-1α, whereas cyclin D1 and Glut-1 are regulated by HIF-2α. Furthermore, erythropoietin was shown to be a HIF-2α target gene.[45] Our microarray analysis and qPCR suggest that renal protection was mainly conferred through HIF-1.

The observation that tubular changes are mainly sublethal 24 hours after the onset of rhabdomyolysis is in line with the limited tubular injury seen in human AKI.[3,46] Such potentially reversible injury opens a window of opportunity for renal protection. Our study focuses on this time span of already detectable and progressive pathology, which precedes necrosis by roughly 1 day. We hypothesized that the transcriptome would allow detection of HIF-related renal-protective mechanisms at this stage.

This study aimed to separately assess the transcriptome in VHL-KO, AKI, and their combination. AKI *per se* has a deep effect on gene regulation, affecting nearly 20% of the active genome. VHL-KO *per se*, which was previously shown to produce no major renal pathology,[34] regulates approximately 3% of the active genome. Interestingly, VHL-KO superimposed on AKI causes a unique HIF transcriptome. Thus, of 1167 upregulated genes in VHL-KO/AKI (Figure 8B), 518 were neither shared with AKI nor with VHL-KO *per se*. Epigenetics may explain this phenomenon, at least in part. The balance between histone acetylases and demethylases is altered by hypoxia; hence, new HREs may become accessible for HIF in AKI.[47,48]

The number of acknowledged HIF target genes exceeds 350,[31] giving rise to a myriad of possible biologic effects. Thus far, no study has systematically investigated the genome under HIF activation *and* established AKI. Our study shows a significant association between renal protection and a shift of energy metabolism. We provide evidence for a HIF-orchestrated program that comprises increased cellular glucose uptake and utilization, autophagy, gluconeogenesis, glycolysis, proton removal, vasodilation, as well as decreased fatty acid utilization and aerobe ATP production. Under oxygen shortage, it is biochemically advantageous to reduce oxygen-dependent ATP production, and to expand oxygen-independent, although less efficient, glycolysis.[32,49] To match increased glucose consumption, at least two mechanisms are intensified: uptake from the environment and gluconeogenesis. As a major drawback, glycolysis may lead to acidosis unless powerful proton excretion devices are provided. *De novo* expression of Car-9 in the basolateral membrane of proximal tubules indicates that proton excretion *via* the blood stream may be part of the HIF-mediated rescue mechanism.

Mitochondria may become sources of apoptosis and necrosis signals in hypoxia.[50] In this context autophagy can help to remove damaged and potentially harmful mitochondria,[51] and at the same time provide new substrates for glycolysis. Bnip3, one of the top 30 upregulated genes in VHL-KO/AKI versus AKI (Table 4), promotes either apoptosis or autophagy, the latter being largely specific for mitochondria.[52] Although microarray analysis revealed enhanced Bnip3 in VHL-KO versus controls, as well as in VHL-KO/AKI versus AKI, the apoptosis marker Casp-3 was increased in the former but decreased in the latter (Figure 6). It is tempting to assume that Bnip3 action depends on the underlying condition, promoting apoptosis in normoxia but repressing it under hypoxic conditions. In the setting of VHL-KO/AKI, additional HIF-dependent factors may repress apoptosis, as recently demonstrated for the glycolytic key enzyme Hk-2.[53]

Of note, the TNF/NF-κB pathway was the most significantly upregulated during AKI, and VHL-KO/AKI significantly reduced the inflammatory transcripts TNF-1α, TNF-1β, IL-1β, and IL-6, as assessed by microarray analysis. Whether this is a direct effect of VHL-KO/HIF activation, or a consequence of reduced tubular necrosis, requires further investigation.

Our data strongly suggest that proximal tubules overexpressing HIF are protected from acute injury. However, Schley *et al.*[54] showed that selective VHL deletion in thick ascending limbs ameliorates ischemic proximal tubular damage. Although the mechanisms responsible for such remote protection of proximal tubules remain elusive, they may operate in Pax8-rtTA–based VHL-KO mice as well. Our data do not exclude that extratubular or HIF-independent mechanisms have the potential to ameliorate AKI. Recent studies indicate that

blood-borne infiltrating cells play an important role in kidney protection.[55,56] In rhabdomyolysis, the cell-protective enzyme Hmox-1 is upregulated in renal proximal tubules[16,57] in the absence of HIF.[16]

In conclusion, a genome-wide search for potentially renal-protective genes in early stages after the onset of AKI provides strong evidence for a metabolic shift toward anaerobic energy metabolism in tubules at risk as the main mechanism of renal protection through VHL knockout.

CONCISE METHODS

Animals

Mice of both sexes (24–31 g body weight) were fed a standard rodent chow with 19% protein content (V1534/300; Ssniff, Soest, Germany) and had free access to drinking water unless otherwise specified. Up to five mice were housed per cage in 12-hour day and night cycles. All experiments were carried out in transgenic mice in which selective renal tubular VHL-KO was inducible by doxycycline.[34] Animal care and treatment were in conformity with the guidelines of the American Physiologic Society, and were also approved by the Berlin Senate (G0014/07).

Experimental Protocols

Four groups of animals were used: (*1*) controls, n=10 untreated mice; (*2*) VHL-KO, n=10 injected with doxycycline (0.1 mg per 10 g body weight subcutaneously) 4 days before euthanasia; (*3*) AKI, n=24 with rhabdomyolysis; and (*4*) VHL-KO/AKI, n=24 with rhabdomyolysis injected with doxycycline (Figure 1). To induce AKI, 50% glycerol (0.05 ml per 10 g body weight) was injected intramuscularly into the left hind limb under inhalation narcosis. Drinking water was withdrawn between 20 hours before and 24 hours after glycerol injection. Before glycerol injection and at either 24 hours or 48 hours thereafter, animals had blood collections from the facial vein[58] for creatinine and urea, which were determined using a Roche Cobas modular PPP-800. The kidneys were then harvested.

Organ Harvesting and Fixation

For each condition, half of the animals had their kidneys fixed by perfusion under deep pentobarbital anesthesia.[59] The other half had their kidneys harvested after cervical dislocation under inhalation anesthesia, and either fixed by immersion or processed for homogenization. The fixation protocol included 3% paraformaldehyde and 1.5% glutaraldehyde/1.5% paraformaldehyde postfixation for semithin analysis and electron microscopy. Solutions were buffered with Na-cacodylate buffer.[59] After fixation, specimens were transferred to 330 mOsmol/L^{-1} sucrose in PBS with 0.02% sodium azide. Later, specimens were further prepared and either embedded in paraffin or Epon and sectioned according to a standard protocol.[59] Tissue homogenates were performed from transversally sectioned fresh kidney halves that were snap frozen in liquid nitrogen immediately thereafter.

Morphologic Studies

Rhabdomyolysis leads to injury mainly in proximal tubules.[60] Three categories of acute tubular injury were defined in 0.5-μm semithin sections, but were equally detectable in 2-μm paraffin sections stained with periodic acid–Schiff, which served for semiquantitative scoring. Each proximal tubular profile was assigned to one of the following categories on the basis of the highest grade injury: 0, unremarkable (any changes not fitting into the subsequent categories); I, vacuoles of more than half of a nuclear diameter; II, flattening with tubular cytoplasmic height (excluding brush border) of less than half of normal; and III, necrosis. Proximal tubular injury in the cortex was semiquantitatively assessed by point counting at $\times$400 magnification using a grid. At least 200 proximal tubular profiles were counted per animal.

Immunohistochemistry was performed on paraffin sections as previously described.[25] The following primary antisera were used: rabbit anti-human HIF-1α (#10006421, 1:30,000; Cayman Chemical, Ann Arbor, MI), rabbit anti-mouse HIF-2α (PM9, 1:12,500; gift from Patrick Maxwell, Imperial College, London, UK), rabbit anti-human glucose transporter-1 (Glut-1, #GT12-A, 1:10,000; Biotrend, Cologne, Germany), and rabbit anti-human carbonic anhydrase-9 (Car-9, #NB100–417, 1:10,000; Novus Biologicals, Littleton, CO). Semiquantitative scores for tubular HIF-1α and HIF-2α were performed by estimating three grades of histochemical signal: + was assigned to a proportion of less than one third of tubular profiles, ++ to one third to two thirds, and +++ to more than two thirds. For tubulointerstitial HIF-2α, + was assigned to a proportion of $<$5 signals per $\times$100 magnification field, ++ to 6–10, and +++ to $>$10. Light microscopy was performed with the help of a Leica DMRB fluorescence microscope equipped with an interference contrast module (Leica, Wetzlar, Germany). Images were acquired using a SPOT RT 2.3.0 digital camera (Diagnostic Instruments, Sterling Heights, MI) and the MetaVue imaging system (Molecular Devices, Downingtown, PA).

Western Blot Analyses

To determine caspase-3 protein levels, extracts from kidneys were prepared as previously described.[61] Proteins were separated by SDS-PAGE and transferred to Hybond-P membranes. Caspase-3 protein was detected using a specific antibody (#AM08377PU-N; Acris Antibodies GmbH, Herford, Germany) and secondary antibody goat-anti-mouse (#sc2031, dilution 1:100,000; Santa Cruz Biotechnology, Santa Cruz, CA). Detection of relative class IIb β-tubulin protein levels served as a loading control (primary antibody: anti-Tubb2B, #10063-2-AP, dilution 1:1000, Proteintech, Chicago, IL) (secondary antibody: donkey anti-rabbit, #sc2317, dilution 1:100,000; Santa Cruz Biotechnology).

Microarray Analyses

Controls (n=3) were compared with VHL-KO (n=3), AKI at day 1 (n=5), and VHL-KO/AKI at day 1 (n=5). Total RNA from halved kidneys was isolated using RNA-Bee (AMS Biotechnology Ltd, Lake Forest, CA) according to the manufacturer's instructions. RNA integrity was checked by analyzing on the 2100 Bioanalyzer (Agilent Technologies, Santa Clara, CA). For global gene expression profile analysis, the Affymetrix Mouse Gene 1.0ST Array (Affymetrix Inc., Santa Clara, CA) was used according to the manufacturer's recommendations. Arrays were processed at the Charité Genome Analysis Facility. Logarithm to the basis 2 (LOG2) levels of signal intensities were considered to be present when values were $>$6 in expressed

genes. Data and relevant information can be accessed at the Gene Expression Omnibus database (accession number: GSE44925).

Functional Enrichment Analyses

Microarray data served for functional enrichment analysis using the Web-based Gene Set Analysis Toolkit (WebGestalt).[62,63] Enrichment analysis of gene sets that were either significantly upregulated or downregulated in VHL-KO animals and/or AKI was performed based on the Gene Ontology, KEGG Pathway, and WikiPathways databases. To ensure high stringency, we selected groups according to a P value <0.01.

mRNA Quantification

RNA was isolated using RNA-Bee (AMS Biotechnology Europe Ltd) according to the manufacturer's instructions and was reverse transcribed using Superscript and random hexamers (Invitrogen, Darmstadt, Germany). qPCR analysis was performed using SYBR Green master mix in a GeneAmp 5700 (Applied Biosystems). Two microliters of cDNA corresponding to 20 ng RNA served as a template. Primers were designed to bridge at least one intron. The primer sequences used for PCR amplification are presented in Supplemental Table 1. The following genes were tested: adrenomedullin (Adm; NM_009627.1), carbonic anhydrase 9 (Car-9, NM_139305.2), hexokinase-2 (Hk2, NM_013820.3), aldolase-C, fructose-bisphosphatase (AldoC, NM_009657.3), solute carrier family 2 (facilitated glucose transporter), member 1 (Slc2a1 [Glut-1], NM_011400.3), and heme oxygenase (decycling) 1 (Hmox-1, NM_010442.2). The expression levels were calculated according to the ΔCt-method with 18S rRNA as the reference gene. Parallelism of standard curves of the test and control was confirmed.

Statistical Analyses

Data are presented as the mean ± SD. At least six animals were analyzed in each experimental group, unless otherwise specified. Data were analyzed by the unpaired t test or Mann–Whitney U test where appropriate. A P value <0.05 was considered statistically significant.

ACKNOWLEDGMENTS

The authors thank Kerstin Riskowsky, Petra Schrade, Jeannette Werner, and John Horn for their skillful assistance.

This study was supported by the German Research Foundation (FOR 1368, DFG).

DISCLOSURES

None.

REFERENCES

1. Waikar SS, Liu KD, Chertow GM: Diagnosis, epidemiology and outcomes of acute kidney injury. *Clin J Am Soc Nephrol* 3: 844–861, 2008
2. Hoste EAJ, Schurgers M: Epidemiology of acute kidney injury: How big is the problem? *Crit Care Med* 36[Suppl]: S146–S151, 2008
3. Kellum JA: Acute kidney injury. *Crit Care Med* 36[Suppl]: S141–S145, 2008
4. Coca SG, Yusuf B, Shlipak MG, Garg AX, Parikh CR: Long-term risk of mortality and other adverse outcomes after acute kidney injury: A systematic review and meta-analysis. *Am J Kidney Dis* 53: 961–973, 2009
5. Huerta-Alardín AL, Varon J, Marik PE: Bench-to-bedside review: Rhabdomyolysis — an overview for clinicians. *Crit Care* 9: 158–169, 2005
6. Malinoski DJ, Slater MS, Mullins RJ: Crush injury and rhabdomyolysis. *Crit Care Clin* 20: 171–192, 2004
7. Vanholder R, Sever MS, Erek E, Lameire N: Rhabdomyolysis. *J Am Soc Nephrol* 11: 1553–1561, 2000
8. Khan FY: Rhabdomyolysis: A review of the literature. *Neth J Med* 67: 272–283, 2009
9. Oken DE: Acute renal failure (vasomotor nephropathy): Micropuncture studies of the pathogenetic mechanisms. *Annu Rev Med* 26: 307–319, 1975
10. Oken DE, Arce ML, Wilson DR: Glycerol-induced hemoglobinuric acute renal failure in the rat. I. Micropuncture study of the development of oliguria. *J Clin Invest* 45: 724–735, 1966
11. Oken DE, DiBona GF, McDonald FD: Micropuncture studies of the recovery phase of myohemoglobinuric acute renal failure in the rat. *J Clin Invest* 49: 730–737, 1970
12. Ayer G, Grandchamp A, Wyler T, Truniger B: Intrarenal hemodynamics in glycerol-induced myohemoglobinuric acute renal failure in the rat. *Circ Res* 29: 128–135, 1971
13. Hsu CH, Kurtz TW, Sands CE: Intrarenal vascular resistance in glycerol-induced acute renal failure in the rat. *Circ Res* 45: 583–587, 1979
14. Wolfert AI, Oken DE: Glomerular hemodynamics in established glycerol-induced acute renal failure in the rat. *J Clin Invest* 84: 1967–1973, 1989
15. Milman Z, Heyman SN, Corchia N, Edrei Y, Axelrod JH, Rosenberger C, Tsarfati G, Abramovitch R: Hemodynamic response magnetic resonance imaging: Application for renal hemodynamic characterization. *Nephrol Dial Transplant* 28: 1150–1156, 2013
16. Rosenberger C, Goldfarb M, Shina A, Bachmann S, Frei U, Eckardt KU, Schrader T, Rosen S, Heyman SN: Evidence for sustained renal hypoxia and transient hypoxia adaptation in experimental rhabdomyolysis-induced acute kidney injury. *Nephrol Dial Transplant* 23: 1135–1143, 2008
17. Flögel U, Merx MW, Gödecke A, Decking UK, Schrader J: Myoglobin: A scavenger of bioactive NO. *Proc Natl Acad Sci U S A* 98: 735–740, 2001
18. Schaad O, Zhou HX, Szabo A, Eaton WA, Henry ER: Simulation of the kinetics of ligand binding to a protein by molecular dynamics: Geminate rebinding of nitric oxide to myoglobin. *Proc Natl Acad Sci U S A* 90: 9547–9551, 1993
19. Holt S, Moore K: Pathogenesis of renal failure in rhabdomyolysis: The role of myoglobin. *Exp Nephrol* 8: 72–76, 2000
20. Nangaku M, Rosenberger C, Heyman SN, Eckardt KU: Regulation of hypoxia-inducible factor in kidney disease. *Clin Exp Pharmacol Physiol* 40: 148–157, 2013
21. Gross MW, Karbach U, Groebe K, Franko AJ, Mueller-Klieser W: Calibration of misonidazole labeling by simultaneous measurement of oxygen tension and labeling density in multicellular spheroids. *Int J Cancer* 61: 567–573, 1995
22. Rosenberger C, Heyman SN, Rosen S, Shina A, Goldfarb M, Griethe W, Frei U, Reinke P, Bachmann S, Eckardt KU: Up-regulation of HIF in experimental acute renal failure: Evidence for a protective transcriptional response to hypoxia. *Kidney Int* 67: 531–542, 2005
23. Yasuda H, Yuen PS, Hu X, Zhou H, Star RA: Simvastatin improves sepsis-induced mortality and acute kidney injury via renal vascular effects. *Kidney Int* 69: 1535–1542, 2006
24. Heyman SN, Rosenberger C, Rosen S: Experimental ischemia-reperfusion: Biases and myths-the proximal vs. distal hypoxic tubular injury debate revisited. *Kidney Int* 77: 9–16, 2010
25. Rosenberger C, Mandriota S, Jürgensen JS, Wiesener MS, Hörstrup JH, Frei U, Ratcliffe PJ, Maxwell PH, Bachmann S, Eckardt KU: Expression of

hypoxia-inducible factor-1alpha and -2alpha in hypoxic and ischemic rat kidneys. *J Am Soc Nephrol* 13: 1721–1732, 2002
26. Maxwell PH: HIF-1's relationship to oxygen: Simple yet sophisticated. *Cell Cycle* 3: 156–159, 2004
27. Metzen E, Ratcliffe PJ: HIF hydroxylation and cellular oxygen sensing. *Biol Chem* 385: 223–230, 2004
28. Semenza GL: Hydroxylation of HIF-1: Oxygen sensing at the molecular level. *Physiology (Bethesda)* 19: 176–182, 2004
29. Wenger RH, Stiehl DP, Camenisch G: Integration of oxygen signaling at the consensus HRE. *Sci STKE* 2005: re12, 2005
30. Ortiz-Barahona A, Villar D, Pescador N, Amigo J, del Peso L: Genome-wide identification of hypoxia-inducible factor binding sites and target genes by a probabilistic model integrating transcription-profiling data and in silico binding site prediction. *Nucleic Acids Res* 38: 2332–2345, 2010
31. Schödel J, Mole DR, Ratcliffe PJ: Pan-genomic binding of hypoxia-inducible transcription factors. *Biol Chem* 394: 507–517, 2013
32. Semenza GL: HIF-1 mediates the Warburg effect in clear cell renal carcinoma. *J Bioenerg Biomembr* 39: 231–234, 2007
33. Kaelin WG Jr: The von Hippel-Lindau tumour suppressor protein: O_2 sensing and cancer. *Nat Rev Cancer* 8: 865–873, 2008
34. Mathia S, Paliege A, Koesters R, Peters H, Neumayer HH, Bachmann S, Rosenberger C: Action of hypoxia-inducible factor in liver and kidney from mice with Pax8-rtTA-based deletion of von Hippel-Lindau protein. *Acta Physiol (Oxf)* 207: 565–576, 2013
35. Aukland K, Krog J: Renal oxygen tension. *Nature* 188: 671, 1960
36. Leichtweiss HP, Lübbers DW, Weiss C, Baumgärtl H, Reschke W: The oxygen supply of the rat kidney: Measurements of intrarenal pO2. *Pflugers Arch* 309: 328–349, 1969
37. Evans RG, Gardiner BS, Smith DW, O'Connor PM: Intrarenal oxygenation: Unique challenges and the biophysical basis of homeostasis. *Am J Physiol Renal Physiol* 295: F1259–F1270, 2008
38. Semenza GL, Roth PH, Fang H-M, Wang GL: Transcriptional regulation of genes encoding glycolytic enzymes by hypoxia-inducible factor 1. *J Biol Chem* 269: 23757–23763, 1994
39. Chen C, Pore N, Behrooz A, Ismail-Beigi F, Maity A: Regulation of glut1 mRNA by hypoxia-inducible factor-1. Interaction between H-ras and hypoxia. *J Biol Chem* 276: 9519–9525, 2001
40. Holotnakova T, Ziegelhoffer A, Ohradanova A, Hulikova A, Novakova M, Kopacek J, Pastorek J, Pastorekova S: Induction of carbonic anhydrase IX by hypoxia and chemical disruption of oxygen sensing in rat fibroblasts and cardiomyocytes. *Pflugers Arch* 456: 323–337, 2008
41. Cormier-Regard S, Nguyen SV, Claycomb WC: Adrenomedullin gene expression is developmentally regulated and induced by hypoxia in rat ventricular cardiac myocytes. *J Biol Chem* 273: 17787–17792, 1998
42. Lee PJ, Jiang BH, Chin BY, Iyer NV, Alam J, Semenza GL, Choi AM: Hypoxia-inducible factor-1 mediates transcriptional activation of the heme oxygenase-1 gene in response to hypoxia. *J Biol Chem* 272: 5375–5381, 1997
43. Pastoreková S, Parkkila S, Parkkila AK, Opavský R, Zelník V, Saarnio J, Pastorek J: Carbonic anhydrase IX, MN/CA IX: Analysis of stomach complementary DNA sequence and expression in human and rat alimentary tracts. *Gastroenterology* 112: 398–408, 1997
44. Raval RR, Lau KW, Tran MG, Sowter HM, Mandriota SJ, Li JL, Pugh CW, Maxwell PH, Harris AL, Ratcliffe PJ: Contrasting properties of hypoxia-inducible factor 1 (HIF-1) and HIF-2 in von Hippel-Lindau-associated renal cell carcinoma. *Mol Cell Biol* 25: 5675–5686, 2005
45. Warnecke C, Zaborowska Z, Kurreck J, Erdmann VA, Frei U, Wiesener M, Eckardt KU: Differentiating the functional role of hypoxia-inducible factor (HIF)-1alpha and HIF-2alpha (EPAS-1) by the use of RNA interference: Erythropoietin is a HIF-2alpha target gene in Hep3B and Kelly cells. *FASEB J* 18: 1462–1464, 2004
46. Rosen S, Stillman IE: Acute tubular necrosis is a syndrome of physiologic and pathologic dissociation. *J Am Soc Nephrol* 19: 871–875, 2008
47. Brigati C, Banelli B, di Vinci A, Casciano I, Allemanni G, Forlani A, Borzì L, Romani M: Inflammation, HIF-1, and the epigenetics that follows. *Mediators Inflamm* 2010: 263914, 2010
48. Luo W, Chang R, Zhong J, Pandey A, Semenza GL: Histone demethylase JMJD2C is a coactivator for hypoxia-inducible factor 1 that is required for breast cancer progression. *Proc Natl Acad Sci U S A* 109: E3367–E3376, 2012
49. Goda N, Kanai M: Hypoxia-inducible factors and their roles in energy metabolism. *Int J Hematol* 95: 457–463, 2012
50. Gustafsson AB: Bnip3 as a dual regulator of mitochondrial turnover and cell death in the myocardium. *Pediatr Cardiol* 32: 267–274, 2011
51. Periyasamy-Thandavan S, Jiang M, Schoenlein P, Dong Z: Autophagy: Molecular machinery, regulation, and implications for renal pathophysiology. *Am J Physiol Renal Physiol* 297: F244–F256, 2009
52. Bruick RK: Expression of the gene encoding the proapoptotic Nip3 protein is induced by hypoxia. *Proc Natl Acad Sci U S A* 97: 9082–9087, 2000
53. Gall JM, Wong V, Pimental DR, Havasi A, Wang Z, Pastorino JG, Bonegio RG, Schwartz JH, Borkan SC: Hexokinase regulates Bax-mediated mitochondrial membrane injury following ischemic stress. *Kidney Int* 79: 1207–1216, 2011
54. Schley G, Klanke B, Schödel J, Forstreuter F, Shukla D, Kurtz A, Amann K, Wiesener MS, Rosen S, Eckardt KU, Maxwell PH, Willam C: Hypoxia-inducible transcription factors stabilization in the thick ascending limb protects against ischemic acute kidney injury. *J Am Soc Nephrol* 22: 2004–2015, 2011
55. Wei Q, Hill WD, Su Y, Huang S, Dong Z: Heme oxygenase-1 induction contributes to renoprotection by G-CSF during rhabdomyolysis-associated acute kidney injury. *Am J Physiol Renal Physiol* 301: F162–F170, 2011
56. Zhang MZ, Yao B, Yang S, Jiang L, Wang S, Fan X, Yin H, Wong K, Miyazawa T, Chen J, Chang I, Singh A, Harris RC: CSF-1 signaling mediates recovery from acute kidney injury. *J Clin Invest* 122: 4519–4532, 2012
57. Nath KA, Haggard JJ, Croatt AJ, Grande JP, Poss KD, Alam J: The indispensability of heme oxygenase-1 in protecting against acute heme protein-induced toxicity in vivo. *Am J Pathol* 156: 1527–1535, 2000
58. University of Minnesota Research Animal Resources: Facial vein technique: How to obtain blood samples from the facial vein of a mouse. Available at: http://www.ahc.umn.edu/rar/facial_vein.html. Accessed August 4, 2013
59. Bachmann S, Kriz W: Histotopography and ultrastructure of the thin limbs of the loop of Henle in the hamster. *Cell Tissue Res* 225: 111–127, 1982
60. Zager RA, Foerder C, Bredl C: The influence of mannitol on myoglobinuric acute renal failure: Functional, biochemical, and morphological assessments. *J Am Soc Nephrol* 2: 848–855, 1991
61. Lai EY, Martinka P, Fähling M, Mrowka R, Steege A, Gericke A, Sendeski M, Persson PB, Persson AE, Patzak A: Adenosine restores angiotensin II-induced contractions by receptor-independent enhancement of calcium sensitivity in renal arterioles. *Circ Res* 99: 1117–1124, 2006
62. Zhang B, Kirov SA, Snoddy JR: WebGestalt: An integrated system for exploring gene sets in various biological contexts. *Nucleic Acids Res* 33: W741–W748, 2005
63. Duncan DT, Prodduturi N, Zhang B: WebGestalt2: An updated and expanded version of the Web-based Gene Set Analysis Toolkit. *BMC Bioinformatics* 11[Suppl 4]: 10, 2010

This article contains supplemental material online at http://jasn.asnjournals.org/lookup/suppl/doi:10.1681/ASN.2013030281/-/DCSupplemental.

7. Lebenslauf

"Mein Lebenslauf wird aus datenschutzrechtlichen Gründen in der elektronischen Version meiner Arbeit nicht veröffentlicht."

Publikationsliste

Stand Januar 2014

1. Ebbing J, **Mathia S**, Seibert FS, Pagonas N, Bauer F, Erber B, Günzel K, Kilic E, Kempkensteffen C, Miller K, Bachmann A, Rosenberger C, Zidek W, Westhoff TH. Urinary calprotectin: a new diagnostic marker in urothelial carcinoma of the bladder. World J Urol. 2013 Dec 31. [Epub ahead of print]
   Impact Factor 2.888

2. Koeners MP, Vink EE, Kuijper A, Gadellaa N, Rosenberger C, **Mathia S**, van den Meiracker AH, Garrelds IM, Blankestijn PJ, Joles JA. Stabilization of hypoxia inducible factor-1α ameliorates acute renal neurogenic hypertension. J Hypertens. 2013 Dec 4. [Epub ahead of print]
   Impact Factor 3.806

3. Fähling M, **Mathia S**, Paliege A, Koesters R, Mrowka R, Peters H, Persson PB, Neumayer HH, Bachmann S, Rosenberger C. Tubular von Hippel-Lindau knockout protects against rhabdomyolysis-induced AKI. J Am Soc Nephrol. 2013 Nov;24(11):1806-19. doi: 10.1681/ASN.2013030281. Epub 2013 Aug 22.
   Impact Factor 8.987

4. **Mathia S**, Paliege A, Koesters R, Peters H, Neumayer HH, Bachmann S, Rosenberger C. Action of hypoxia-inducible factor in liver and kidney from mice with Pax8-rtTA-based deletion of von Hippel-Lindau protein. Acta Physiol (Oxf). 2013 Mar;207(3):565-76. doi: 10.1111/apha.12058.
   Impact Factor 4.382

5. Dietrich A, **Mathia S**, Kaminski H, Mutig K, Rosenberger C, Mrowka R, Bachmann S, Paliege A. Chronic activation of vasopressin V2 receptor signalling lowers renal medullary oxygen levels in rats. Acta Physiol (Oxf). 2013 Apr;207(4):721-31. doi: 10.1111/apha.12067. Epub 2013 Feb 18.
   Impact Factor 4.382

6. Stricker S, **Mathia S**, Haupt J, Seemann P, Meier J, Mundlos S. Odd-skipped related genes regulate differentiation of embryonic limb mesenchyme and bone marrow mesenchymal stromal cells. Stem Cells Dev. 2012 Mar 1;21(4):623-33. doi: 10.1089/scd.2011.0154. Epub 2011 Jul 26.
   Impact Factor 4.670

7. Hufton AL, **Mathia S**, Braun H, Georgi U, Lehrach H, Vingron M, Poustka AJ, Panopoulou G. Deeply conserved chordate noncoding sequences preserve genome synteny but do not drive gene duplicate retention. Genome Res. 2009 Nov;19(11):2036-51. doi: 10.1101/gr.093237.109. Epub 2009 Aug 24.
   Impact Factor 14.397

Die Publikationen 1-5 sind im Rahmen der Dissertation entstanden.

8. Danksagung

Besonders herzlich möchte ich mich bei meinem Doktorvater PD Dr. med. Christian Rosenberger bedanken, denn er stand mir immer mit Rat und Tat zur Seite. Ich kann mich gar nicht oft genug dafür bedanken, dass ich dieses außerordentlich spannende Thema bearbeiten durfte, für die zahlreiche Ideen und konstruktive Kritik und die vielen Emails zur Beantwortung meiner Fragen auch noch zu später Stunde, für die immerwährende Unterstützung und den mir eingeräumten Freiraum. Danke!

Auch danke ich Herrn Prof. Dr. Bachmann und seiner Arbeitsgruppe im Institut für vegetative Anatomie an der Charité für die Zusammenarbeit und die allwöchentlichen Diskussionsrunden. Besonderer Dank geht an Kerstin Riskowsky für Ihren Rat bezüglich der Immunhistochemie und Probenvorbereitung. Vielen Dank an Petra Schrade und John Horn für eure Mitarbeit.

Des Weiteren möchte ich mich ganz herzlich bei Prof. Dr. Michael Fähling und Prof. Dr. Andreas Patzak bedanken, denn ich habe bei einer Tasse Kaffee und einem netten Gespräch des Öfteren eine gute Idee bekommen, um knifflige technische Probleme zu lösen. Vielen Dank auch an Jeannette Werner für die stetige Hilfe bei den molekularbiologischen Methoden.

Vielen Dank an Dr. Alexander Paliege, Prof. Dr. Robert Koesters, Prof. Dr. Ralf Mrowka, Prof. Dr. Harm Peters, Prof. Dr. Pontus Börje Persson und Prof. Dr. Hans-Hellmut Neumayer für die Mitarbeit an der dieser Dissertation zugrunde liegenden Publikation.

Allen Mitarbeitern des Center for Cardiovascular Research (CCR) der Charité danke ich für das freundliche und angenehme Arbeitsklima in unserem Haus. Vielen Dank, dass ich mir hin und wieder ein paar Kleinigkeiten ausleihen durfte. Vielen Dank an die Tierpfleger des CCRs, denn ohne deren fleißigen Einsatz wären die Experimente nicht machbar gewesen.

Vielen Dank an alle!